

# Discretization methods with analytical solutions for a convection-diffusion-dispersion-reaction- equations and applications in 2D and 3D for waste-scenarios. \*

Jürgen Geiser

Institut of Computer Science,  
Im Neuenheimer Feld 368, D-69120 Heidelberg, Germany  
juergen.geiser@iwr.uni-heidelberg.de

**Abstract.** In this part we describe the numerical methods and the results for our discretization methods for system of convection-diffusion-dispersion-reaction equation. The motivation came for the simulation of a scenario of a waste-disposal done over a large time-periods. For the methods large time-steps should be allowed to reach the large simulation periods of 10000 years. The idea is to use higher order discretization methods which allows large time-steps without lost of accuracy. We decouple a multi-physical multidimensional equation in simpler physical and one-dimensional equations. These simpler equations are handled with higher order discretization and the results are coupled with an operator-splitting method together. We describe the discretization methods for the convection-reaction equation and for the diffusion-dispersion equation. Both are based on vertex centered finite volume methods. For the convection-reaction equation a modified discretization method with embedded analytical solutions is presented. To couple the simpler equations the operator splitting method is presented with respect to the splitting-errors of the method. The higher order splitting methods are further presented. The underlying program-tool  $R^3T$  is brief introduced and the main concepts are presented. We introduce the benchmark problems for testing the modified discretization methods of higher order. A new model problem of a rotating pyramid with analytical solutions is discussed as a benchmark problem for two dimensional problems. The complex problems for the simulation of radioactive waste disposals with underlying flowing groundwater are further presented. The transport and reaction simulations for decay chains are presented in 2d and 3d domains. The results of this calculations are discussed. The further works are introduced and conclusions are derived from the work.

## 1 Introduction

Our motivation for studying the transport-reaction processes came from the background of the simulation of waste-disposals for radioactive contaminants

---

\* This work is funded by the Federal Ministry of Economics and Technology (BMWi) under the contract number 02 E 9148 2

transported with flowing groundwater through an overlying rock. For this model the derivation of the equations are done. We have the aim to describe the solving of the equations based on the discretization methods for the convection dominant case. For the discretization we introduce the decoupling methods. We split the complex and multidimensional equation in simpler equations. The operator-splitting method is based on a first order splitting. We could increase the order by using a higher order splitting method. Our problem is so posed, that we have dominant error in space, because of coarse grids for the discretization, therefore higher order methods in space are necessary. The time-error, even coming from a first order method does not influence our spatial-error. So the discretization methods are important and are adapted to the equations. For the convection-reaction equation we use explicit time-discretizations and higher order finite volume methods for the space-discretization. An improved higher order discretization method for the convection-reaction equation is presented and for this method the splitting-error in time is skipped. The method is based on an analytical solution for the convection-reaction equation in the one-dimensional case. This discretization reduce the amount of artificial diffusion. For the diffusion-dispersion equation we use implicit time-discretization and the finite volume methods for the space-discretizations. For both discretization methods we receive a higher order method. The solvers for the implicit methods are done with multi-grid-solvers as pre-conditioners. The methods are programmed and applicable in the software package  $R^3T$ . The program concepts are introduce. We applied our methods for Benchmark-problems which are based on analytical solutions. A new benchmark problem for two and three dimensions for a contaminant transport and reaction through a complex domain spooled with groundwater is presented. We describe the complex examples for a large decay-chain and a complex domain flowing through with a groundwater. The velocities of the groundwater is calculated with a software tool  $d^3f$  with flowing equations. The results of the 2d and 3d applications are discussed and presented with different figures.

The paper is organized as follows. A mathematical model of contaminant transport in flowing groundwater is introduced in section 2. The decoupling of the complex equation to physical simpler equations are described in section 3. In section 4 we introduce the discretization methods for the decoupled equations with respect to the convection-reaction equation. The analytical solutions used for the discretization are discussed in the section 5. We introduce the numerical solvers and concentrate us to the multi-grid solver in section 6. We present the software tools in section 7 and our results for the methods in section 8. Finally we discuss our future works in this area of discretization methods.

## 2 Mathematical Model

The motivation for the study presented below is coming from a computational simulation of radionuclide contaminants transport in flowing groundwater [6], [9].

The mathematical equations are given by

$$\partial_t R_\alpha c_\alpha + \nabla \cdot (\mathbf{v}c_\alpha - D\nabla c_\alpha) + \lambda_{\alpha\beta} R_\alpha c_\alpha = \sum_{\gamma \in \gamma(\alpha)} \lambda_{\gamma\alpha} R_\gamma c_\gamma \quad (1)$$

$$\text{with } \alpha = 1, \dots, m \quad (2)$$

The unknowns  $c_\alpha = c_\alpha(x, t)$  are considered in  $\Omega \times (0, T) \subset \mathbb{R}^d \times \mathbb{R}$ , the space-dimension is given by  $d$ . The Parameters  $R_\alpha \in \mathbb{R}^+$  and is constant. and named as retardation factor. The other parameters are  $\lambda_{\alpha\beta}$  the decaying rates from  $\alpha$  to  $\beta$ , whereby  $\gamma(\alpha)$  are the predecessor-elements of element  $\alpha$ .  $D$  is the Scheidegger diffusion-dispersion tensor and  $\mathbf{v}$  is the velocity.

The aim of this paper is to present a new method based on a derived analytical solution of the system of one dimensional convection-reaction equations with different retardation factors and constant velocities combined with an explicit finite volume method for the convection-reaction equations for  $d$  dimensions.

This method has no splitting error and is in the first dimension exact. The idea underly the solving of one dimensional convection-reaction equations and couple them over the mass transport together. So the criteria for large time steps and the use of coarser grids with improved higher order discretization is fulfilled.

The higher order finite volume method based on TVD methods and constructed under the discrete minimum and maximum principle are used for the new methods to reach second order for all components.

For the derivation of the new methods based on the one dimensional analytical solution for convection-reaction-equations we use the  $d$ -dimensional convection-reaction equations with equilibrium sorption.

So the equation is given by:

$$R_i \partial_t c_i + \nabla \cdot (\mathbf{v}c_i) = -\lambda_i R_i c_i + \lambda_{i-1} R_{i-1} c_{i-1}, \quad i = 1, \dots, m, \quad (3)$$

$$c_i = (c_{1,i}, \dots, c_{d,i})^T \in \mathbb{R}^d, \quad (4)$$

whereby the trivial inflow and outflow boundary conditions are given by  $c = 0$  and the initial conditions  $c_i(x, 0) = c_{i,0}(x)$  are given as rectangular-, trapezoidal- and polynomial-impulses are possible. Based on the one dimensional convection-reaction equation with equilibrium sorption and initial impulses, we derive the new discretization methods.

The following section describe the Operator-Splitting method as a method to decouple complex equations to physical simpler equations.

### 3 Operator-Splitting Methods

The operator-splitting methods are used to solve complex models in the geophysical and environmental physics, they are developed and applied in [24], [26] and [29]. We use the ideas for coupling simpler equation parts together, while each space-errors are more dominant then the time-error. That means we could use a first or second order operator splitting that coupled our simpler equation with

larger space-errors together. So we receive higher order in space, the time-error was not important for our coarse grids. For this aim we use the operator-splitting method and decouple the equation as follows described.

### 3.1 Splitting methods of first order

The following splitting methods of first order are described. We consider the following ordinary linear differential equations:

$$\partial_t c(t) = A c(t) + B c(t), \quad (5)$$

whereby the initial-conditions are  $c^n = c(t^n)$ . The operators  $A$  and  $B$  are spatial discretized equations, e.g. the convection-equation and the diffusion-equation.

The operator-splitting method is introduced as a method which solve the two equation-parts sequentially, with respect of the initial conditions. We get two sub-equations :

$$\begin{aligned} \frac{\partial c^*(t)}{\partial t} &= A c^*(t), \quad \text{with } c^*(t^n) = c^n, \\ \frac{\partial c^{**}(t)}{\partial t} &= B c^{**}(t), \quad \text{with } c^{**}(t^n) = c^*(t^{n+1}). \end{aligned} \quad (6)$$

whereby the time-step is  $\tau^n = t^{n+1} - t^n$ . The solution of equations are  $c^{n+1} = c^{**}(t^{n+1})$ .

The error of this splitting method is derived as, confer [14]

$$\begin{aligned} \rho_n &= \frac{1}{\tau} (\exp(\tau^n(A+B)) - \exp(\tau^n B) \exp(\tau^n A)) c(t^n) \\ &= \frac{1}{2} \tau^n [A, B] c(t^n) + O(\tau^2). \end{aligned} \quad (7)$$

whereby  $[A, B] := AB - BA$  is the commutator of  $A$  and  $B$ . We get an error  $O(\tau^n)$  if the Operators  $A$  and  $B$  do not commute, otherwise the method is exact.

### 3.2 Higher order Splitting methods

We could improve our method by the so called Strang-Splitting method, which is of second order, confer [24].

The method is presented as:

$$\begin{aligned} \frac{\partial c^*(t)}{\partial t} &= A c^*(t), \quad \text{with } t^n \leq t \leq t^{n+1/2} \text{ and } c^*(t^n) = c^n, \\ \frac{\partial c^{**}(t)}{\partial t} &= B c^{**}(t), \quad \text{with } t^n \leq t \leq t^{n+1} \text{ and } c^{**}(t^n) = c^*(t^{n+1/2}), \\ \frac{\partial c^{***}(t)}{\partial t} &= A c^{***}(t), \quad \text{with } t^{n+1/2} \leq t \leq t^{n+1} \text{ and } c^{***}(t^{n+1/2}) = c^{**}(t^{n+1/2}), \end{aligned} \quad (8)$$

whereby the results of the method is  $c^{n+1} = c^{***}(t^{n+1})$ .

The splitting error of this method is given as, confer [20]

$$\begin{aligned} \rho_n &= \frac{1}{\tau} (\exp(\tau^n(A+B)) - \exp(\frac{\tau^n}{2}A) \exp(\tau^n B) \exp(\frac{\tau^n}{2}A)) c(t^n) \\ &= \frac{1}{24} (\tau^n)^2 ([B, [B, A]] - 2[A, [A, B]]) c(t^n) + O((\tau^n)^4). \end{aligned} \quad (9)$$

whereby we get the second order if the operators not commute and an exact result if they commute.

We could improve the order by using more intermediate steps. In our application the first order splitting for the convection-reaction- and the diffusion-dispersion-term are applied, because of the dominance of the space-error. The time-error for this combination was only a constant in the total error.

In the next section we present the discretization methods for the equations.

## 4 Discretization

For the space-discretization we use finite volume methods and for the time-discretization we use explicit or implicit Euler methods. In the next section we introduce the notation for the space-discretization. Further we describe the discretization-methods for the further different equation-terms.

### 4.1 Notation

The time steps for the calculation in the time intervals are  $(t^n, t^{n+1}) \subset (0, T)$ , for  $n = 0, 1, \dots$ . The computational cells are given as  $\Omega_j \subset \Omega$  with  $j = 1, \dots, I$ . The unknown  $I$  is the number of the nodes.

For the use of finite volumes we have to construct the dual mesh for the triangulation  $\mathcal{T}$  [11] of the domain  $\Omega$ . First the finite elements for the domain  $\Omega$  are given by  $T^e, e = 1, \dots, E$ . The polygonal computational cells  $\Omega_j$  are related with the vertices  $x_j$  of the triangulation.

To get the relation between the neighbor cells and to use the volume of each cell we introduce the following notation. Let  $V_j = |\Omega_j|$  and the set  $A_j$  denotes the neighbor-point  $x_k$  to the point  $x_j$ . The boundary of the cell  $j$  and  $k$  are  $\Gamma_{jk}$ .

We define the flux over the boundary  $\Gamma_{jk}$  as

$$v_{jk} = \int_{\Gamma_{jk}} \mathbf{n} \cdot \mathbf{v} \, ds. \quad (10)$$

The inflow-flux is given as  $v_{jk} < 0$ , the outflow-flux is  $v_{jk} > 0$ . The antisymmetric of the fluxes are denoted as  $v_{jk} = -v_{kj}$ . The total outflow-flux is given by

$$\nu_j = \sum_{k \in out(j)} v_{jk}. \quad (11)$$

The idea of the finite volumes is to construct an algebraic system of equation to express the unknowns  $c_j^n \approx c(x_j, t^n)$ . The initial values are given with  $c_j^0$ . The expression of the interpolation schemes could be given naturally in two ways, the first is given with the primary mesh of the finite elements:

$$c^n = \sum_{j=1}^I c_j^n \phi_j(x) \quad (12)$$

with  $\phi_j$  are the standard globally finite element basis functions [11]. The second possibility is for the finite volumes with,

$$\hat{c}^n = \sum_{j=1}^I c_j^n \varphi_j(x) \quad (13)$$

where  $\varphi_j$  are piecewise constant discontinuous functions defined by  $\varphi_j(x) = 1$  for  $x \in \Omega_j$  and  $\varphi_j(x) = 0$  otherwise.

#### 4.2 Discretization of the convection-equation with first order

The piecewise constant discretization of the convection equation

$$\partial_t R c - \mathbf{v} \cdot \nabla c = 0, \quad (14)$$

with the simple boundary condition  $c = 0$  for the inflow and outflow boundary and the initial values  $c(x_j, 0) = c_j^0(x)$ . We use the upwind discretization done in [11] and get

$$\begin{aligned} V_j R c_j^{n+1} &= V_j R c_j^n - \tau^n \sum_{k \in \text{out}(j)} v_{jk} c_j^n + \tau^n \sum_{k \in \text{in}(j)} c_k^n v_{kj}, \\ V_j R c_j^{n+1} &= c_j^n (R V_j - \tau^n \nu_j) + \tau^n \sum_{k \in \text{in}(j)} c_k^n v_{kj}, \end{aligned} \quad (15)$$

Because of the explicit discretization for time and to fulfill the discrete minimum-maximum property [11], we get a restriction for the time steps as follows

$$\tau_j = \frac{R V_j}{\nu_j}, \quad \tau^n \leq \min_{j=1, \dots, I} \tau_j \quad (16)$$

In the next subsection we improve the discretization with a reconstruction with linear polynoms. The reconstruction is based on the Godunovs method and the limiter on the local min-max property.

#### 4.3 Discretization of the convection-equation with higher order

The reconstruction is done in the paper [11] and it is here briefly explained for the next steps.

The linear polynomes are reconstruct over the element-wise gradient and are given as

$$u^n(x_j) = c_j^n, \quad (17)$$

$$\nabla u^n|_{V_j} = \frac{1}{V_j} \sum_{e=1}^E \int_{T^e \cap \Omega_j} \nabla c^n dx, \quad (18)$$

with  $j = 1, \dots, I$ .

The piecewise linear function is given by

$$u_{jk}^n = c_j^n + \psi_j \nabla u^n|_{V_j} (x_{jk} - x_j), \quad (19)$$

with  $j = 1, \dots, I$ ,

where  $\psi_j \in (0, 1)$  is the limiter which has to fulfill the discrete minimum maximum property, as described in [11].

We also use the limitation of the flux to get no overshooting, when transporting the mass and receive the maximal time-step.

We get the restriction for the concentration as

$$\tilde{u}_{jk}^n = u_{jk}^n + \frac{\tau_j}{\tau^n} (c_j^n - u_{jk}^n). \quad (20)$$

Using all the previous schemes the discretization for the second order is written in the form

$$RV_j c_j^{n+1} = RV_j c_j^n - \tau^n \sum_{k \in out(j)} \tilde{u}_{jk}^n v_{jk} + \tau^n \sum_{l \in in(j)} \tilde{u}_{lj}^n v_{lj}, \quad (21)$$

This discretization method is used for the next coupled discretization with the reaction equation.

#### 4.4 Discretization of the convection-reaction-equation with one dimensional analytical solutions

We apply Godunovs method for the discretization, confer [22], and enlarge it with the solution of convection-reaction-equations. We reduce the equation to one dimensional problem, solve the equation exactly and transform the one dimensional mass to the multi-dimensional equation.

The discretization of the equation

$$\partial_t c_l + \nabla \cdot \mathbf{v}_l c_l = -\lambda_l c_l + \lambda_{l-1} c_{l-1},$$

with  $l = 1, \dots, m$

The velocity vector  $\mathbf{v}$  is divided by  $R_l$ . The initial conditions are given by  $c_1^0 = c_1(x, 0)$ , else  $c_l^0 = 0$  for  $l = 2, \dots, m$  and the boundary conditions are trivial  $c_l = 0$  for  $l = 1, \dots, m$ .

We first calculate the maximal time step for cell  $j$  and concentration  $i$  with the use of the total outflow fluxes

$$\tau_{i,j} = \frac{V_j R_i}{\nu_j}, \quad \nu_j = \sum_{k \in \text{out}(j)} v_{jk}.$$

We get the restricted time step with the local time steps of cells and their components

$$\tau^n \leq \min_{\substack{i=1,\dots,m \\ j=1,\dots,I}} \tau_{i,j}.$$

The velocity of the discrete equation is given by

$$v_{i,j} = \frac{1}{\tau_{i,j}}.$$

We calculate the analytical solution of the mass, confer section 5 by using equation (42) and (44), we get

$$\begin{aligned} m_{i,jk,\text{out}}^n &= m_{i,\text{out}}(a, b, \tau^n, v_{1,j}, \dots, v_{i,j}, R_1, \dots, R_i, \lambda_1, \dots, \lambda_i), \\ m_{i,j,\text{rest}}^n &= m_{i,j}^n f(\tau^n, v_{1,j}, \dots, v_{i,j}, R_1, \dots, R_i, \lambda_1, \dots, \lambda_i), \end{aligned}$$

whereby  $a = V_j R_i (c_{i,jk}^n - c_{i,jk'}^n)$ ,  $b = V_j R_i c_{i,jk'}^n$  and  $m_{i,j}^n = V_j R_i c_{i,j}^n$  are the parameters. The linear impulse in the finite-volume cell is constructed by  $c_{i,jk'}^n$  for the concentration on the inflow- and  $c_{i,jk}^n$  for the concentration on the outflow-boundary of the cell  $j$ .

The discretization with the embedded analytical mass is calculated by

$$m_{i,j}^{n+1} - m_{i,\text{rest}}^n = - \sum_{k \in \text{out}(j)} \frac{v_{jk}}{\nu_j} m_{i,jk,\text{out}} + \sum_{l \in \text{in}(j)} \frac{v_{lj}}{\nu_l} m_{i,lj,\text{out}},$$

whereby  $\frac{v_{jk}}{\nu_j}$  is the re-transformation for the total mass  $m_{i,jk,\text{out}}$  in the partial mass  $m_{i,jk}$ . The mass in the next time-step is  $m_{i,j}^{n+1} = V_j c_{i,j}^{n+1}$  and in the old time-step it is the rest mass for the concentration  $i$ . The proof is done in [14]. In the next section we derive an analytical solution for the benchmark problem.

#### 4.5 Discretization of the Reaction-equation

The reaction-equation is an ordinary-differential equation is given as follows:

$$\partial_t R_i c_i = -\lambda_i R_i c_i + \lambda_{i-1} R_{i-1} c_{i-1}, \quad (22)$$

whereby  $i = 1, \dots, m$  and  $\lambda_0 = 0$  is. The decay-factors are  $\lambda_i \geq 0.0$  and the retardation-factors are  $R_i > 0.0$ . The initial-conditions are  $c_1(x, t^0) = c_{01}$  and  $c_i(x, t^0) = 0$  with  $i = 2, \dots, m$ .

We could derive the solutions for these equations, confer [3], with:

$$c_i = c_{01} \frac{R_1}{R_i} A_i \sum_{j=1}^i A_{j,i} \exp(-\lambda_j t), \quad (23)$$

whereby  $i = 1, \dots, m$ . The solutions are defined for all  $\lambda_j \neq \lambda_k$  for  $j \neq k$  and  $j, k \in 1, \dots, M$ .

The factors  $A_i$  and  $A_{j,i}$  are

$$A_i = \prod_{j=1}^{i-1} \lambda_j, \quad A_{j,i} = \prod_{\substack{k=1 \\ k \neq j}}^i \frac{1}{\lambda_k - \lambda_j}. \quad (24)$$

For pairwise equal reaction-factors we have derived the solution in our work [14].

In the next subsection we introduce the discretization of the diffusion-dispersion-equation.

#### 4.6 Discretization of the Diffusion-Dispersion-equation

We discretize the diffusion-dispersion-equation with implicit time-discretization and finite volume method for the following equation

$$\partial_t R c - \nabla \cdot (D \nabla c) = 0, \quad (25)$$

whereby  $c = c(x, t)$  with  $x \in \Omega$  and  $t \geq 0$ . The Diffusions-Dispersions-Tensor is  $D = D(x, \mathbf{v})$  given by the Scheidegger-approach, confer [23]. The velocity is given by  $\mathbf{v}$ . The retardation-factor is  $R > 0.0$ .

We have the boundary-values with  $\mathbf{n} \cdot D \nabla c(x, t) = 0$ , whereby  $x \in \Gamma$  is the boundary  $\Gamma = \partial\Omega$ , confer [10]. The initial conditions are given by  $c(x, 0) = c_0(x)$ .

We integrate the equation 25 over space and time and get

$$\int_{\Omega_j} \int_{t^n}^{t^{n+1}} \partial_t R(c) dt dx = \int_{\Omega_j} \int_{t^n}^{t^{n+1}} \nabla \cdot (D \nabla c) dt dx. \quad (26)$$

The integration over time is done with the backward-Euler method and the lumping for the diffusion-dispersion term, confer [14]:

$$\int_{\Omega_j} (R(c^{n+1}) - R(c^n)) dx = \tau^n \int_{\Omega_j} \nabla \cdot (D \nabla c^{n+1}) dx, \quad (27)$$

The equation (27) is discretized over the space with respect of using the Greens-formula.

$$\int_{\Omega_j} (R(c^{n+1}) - R(c^n)) dx = \tau^n \int_{\Gamma_j} D \mathbf{n} \cdot \nabla c^{n+1} d\gamma, \quad (28)$$

whereby  $\Gamma_j$  is the boundary of the finite volume cell  $\Omega_j$ . We use the approximation in space, confer [14].

The integration for the equation (28) is done for finite boundary and by the use of the middle-point rule:

$$V_j R(c_j^{n+1}) - V_j R(c_j^n) = \tau^n \sum_{e \in \Lambda_j} \sum_{k \in \Lambda_j^e} |\Gamma_{jk}^e| \mathbf{n}_{jk}^e \cdot D_{jk}^e \nabla c_{jk}^{e,n+1}, \quad (29)$$

whereby  $|\Gamma_{jk}^e|$  is the length of the boundary-element  $\Gamma_{jk}^e$ . The gradients are calculated with the piecewise finite-element-function  $\phi_l$ , confer equation (12) and we get

$$\nabla c_{jk}^{e,n+1} = \sum_{l \in \Lambda^e} c_l^{n+1} \nabla \phi_l(\mathbf{x}_{jk}^e). \quad (30)$$

We get with the difference-notation for the neighbor-point  $j$  and  $l$ , confer [12], the following discretization form.

$$\begin{aligned} V_j R(c_j^{n+1}) - V_j R(c_j^n) &= \\ &= \tau^n \sum_{e \in \Lambda_j} \sum_{l \in \Lambda^e \setminus \{j\}} \left( \sum_{k \in \Lambda_j^e} |\Gamma_{jk}^e| \mathbf{n}_{jk}^e \cdot D_{jk}^e \nabla \phi_l(\mathbf{x}_{jk}^e) \right) (c_j^{n+1} - c_l^{n+1}), \end{aligned} \quad (31)$$

whereby  $j = 1, \dots, m$ .

In the next section we introduce the analytical solutions for the discretization-methods of the convection-reaction-equation.

## 5 Analytical solutions

For the next section we deal with the following system of one-dimensional convection-reaction-equations without diffusion. The equation is given as

$$\partial_t c_i + v_i \partial_x c_i = -\lambda_i c_i + \lambda_{i-1} c_{i-1}, \quad (32)$$

for  $i = 1, \dots, m$ . The unknown  $m$  is the number of components. The unknown functions  $c_i = c_i(x, t)$  denote the contaminant concentrations. They are transported with piecewise constant (and in general different) velocities  $v_i$ . They decay with constant reaction rates  $\lambda_i$ . The space-time domain is given by  $(0, \infty) \times (0, T)$ .

We assume simple (irreversible) form of decay chain, e.g.  $\lambda_0 = 0$  and for each contaminant only single source term  $\lambda_{i-1} c_{i-1}$  is given. For a simplicity, we assume that  $v_i > 0$  for  $i = 1, \dots, m$ .

We describe the analytical solutions with piecewise linear initial conditions. But all other piecewise polynom functions could be derived, confer [14].

For boundary conditions we take zero concentrations at inflow boundary  $x = 0$  and the initial conditions are defined for  $x \in (0, 1)$  with

$$\begin{aligned} c_1(x, 0) &= \begin{cases} ax + b, & x \in (0, 1) \\ 0 & \text{otherwise} \end{cases}, \\ c_i(x, 0) &= 0, \quad i = 2, \dots, m, \end{aligned} \quad (33)$$

where  $a, b \in \mathbb{R}^+$  are constants.

We use the Laplace-Transformation for the transformation of the partial differential equation into the ordinary differential equation, described in [16]. We solve the ordinary differential equations, described in [5], and re-transformed the solution in the original space of the partial differential equations. We could then use the solution for the one-dimensional convection-reaction-equation, confer [14].

The solutions are given as

$$c_1(x, t) = \exp(-\lambda_1 t) \begin{cases} 0 & 0 \leq x < v_1 t \\ a(x - v_1 t) + b & v_1 t \leq x < v_1 t + 1 \\ 0 & v_1 t + 1 \leq x \end{cases}, \quad (34)$$

$$c_i(x, t) = \Lambda_i \left( \sum_{j=1}^i \exp(-\lambda_j t) \Lambda_{j,i} \sum_{\substack{k=1 \\ k \neq j}}^i \Lambda_{j,k,i} A_{jk} \right), \quad (35)$$

$$A_{jk} = \begin{cases} 0 & 0 \leq x < v_j t \\ a(x - v_j t) \\ + (b - \frac{a}{\lambda_{jk}})(1 - \exp(-\lambda_{jk}(x - v_j t))) & v_j t \leq x < v_j t + 1 \\ (b - \frac{a}{\lambda_{jk}} + a) \exp(-\lambda_{jk}(x - v_j t - 1)) \\ - (b - \frac{a}{\lambda_{jk}}) \exp(-\lambda_{jk}(x - v_j t)) & v_j t + 1 \leq x \end{cases}. \quad (36)$$

where the general solutions have the following definition-array

$v_i \neq v_j$ ,  $\lambda_i \neq \lambda_j$ ,  $\lambda_{ij} \neq \lambda_{ik}$  and  $v_i \neq v_j \wedge \lambda_i \neq \lambda_j$ ,  
 $\forall i, j, k = 1, \dots, M$ , if  $i \neq j \wedge i \neq k \wedge j \neq k$ .

The further abbreviation for  $\lambda_{jk}$  and  $\Lambda_i$  are

$$\lambda_{kj} = \lambda_{jk} := \frac{\lambda_j - \lambda_k}{v_j - v_k}, \quad \Lambda_i := \prod_{j=1}^{i-1} \lambda_j, \quad (37)$$

and the factors  $\Lambda_{j,i}$  and  $\Lambda_{jk,i}$  are

$$\Lambda_{j,i} = \left( \prod_{\substack{k=1 \\ k \neq j}}^i \frac{1}{\lambda_k - \lambda_j} \right), \quad \Lambda_{jk,i} = \left( \prod_{\substack{l=1 \\ l \neq j \\ l \neq k}}^i \frac{1}{\lambda_k - \lambda_l} \right). \quad (38)$$

The solutions (34) and (35) are used in the discretization methods for the embedded analytical mass. In the next subsection we described the mass reconstruction as derived as an analytical solution for the mass.

## 5.1 Mass reconstruction

For the embedding of the analytical mass in the discretization method, we need the mass transfer of the norm-interval  $(0, 1)$ . We use the construction over the

total mass given as

$$m_{i,sum}(t) = m_{i,rest}(t) + m_{i,out}(t) \quad (39)$$

The integrals are computed over the cell  $(0, 1)$ . We integrate first the mass that remain in the cell  $i$  and then we calculate the total mass. The difference between the total mass and the residual mass is the out-flowing mass which is used for the discretization.

The residual mass is described in [14] and given as:

$$m_{i,rest}(t) = \prod_{j=1}^{i-1} \lambda_j \sum_{j=1}^i \left( \prod_{\substack{k=1 \\ k \neq j}}^i \frac{1}{\lambda_k - \lambda_j} \right) \exp(-\lambda_j t) \left( a \frac{(1 - v_j t)^2}{2} + b(1 - v_j t - \sum_{\substack{k=1 \\ k \neq j}}^i \frac{1}{\lambda_{jk}}) - a(1 - v_j t) \left( \sum_{\substack{k=1 \\ k \neq j}}^i \frac{1}{\lambda_{jk}} \right) + a \left( \sum_{\substack{k=1 \\ k \neq j}}^i \frac{1}{\lambda_{jk}} \left( \sum_{\substack{l \geq k \\ l \neq j}}^i \frac{1}{\lambda_{jl}} \right) \right) \right), \quad (40)$$

where the parameters  $\lambda_{jk}$  are given in the equation (37) .

The total mass is calculated by the solution of the ordinary equation and the mass of the initial condition. The solution of the total mass is derived as

$$m_{i,sum}(t) = \prod_{j=1}^{i-1} \lambda_j \left( \sum_{j=1}^i \left( \prod_{\substack{k=1 \\ k \neq j}}^i \frac{1}{\lambda_k - \lambda_j} \right) \exp(-\lambda_j t) \right) \left( \frac{a}{2} + b \right).$$

The out-flowing mass is defined for further calculations

$$m_{i,out}(\tau^n) = m_{i,sum}(\tau^n) - m_{i,rest}(\tau^n), \quad (41)$$

$$m_{i,out}(\tau^n) = m_{i,out}(a, b, \tau^n, v_1, \dots, v_i, R_1, \dots, R_i, \lambda_1, \dots, \lambda_i), \quad (42)$$

$$m_{i,sum}(\tau^n) = f_i^n \left( a \frac{1}{2} + b \right), \quad (43)$$

$$f_i^n(\tau^n) = f(\tau^n, v_1, \dots, v_i, R_1, \dots, R_i, \lambda_1, \dots, \lambda_i). \quad (44)$$

whereby  $\tau^n$  is the time-step,  $v_1, \dots, v_i$  are the velocity-,  $R_1, \dots, R_i$  are the retardation-,  $\lambda_1, \dots, \lambda_i$  the reaction-parameters and  $a, b$  are the parameters for the linear impulse for the initial conditions. In the next section we describe the solver methods used for our computations.

## 6 Solvers

For solving the implicit discretized diffusion-dispersion equation we use iterative methods. We have the full-discretised equation for our diffusion-dispersion equation :

$$(I - \tau \tilde{A})u^{n+1}(\tilde{x}) = u^n(\tilde{x}),$$

where  $\tilde{A}$  is obtained from the spatial discretisation,  $u^{n+1}$  is solution in the new time-step,  $u^n$  is the known solution from the old time-step and  $\tilde{x} \in \Omega_h$ , i.d. the coordinates of the grid-points.

So we deal with a linear equation system  $Ax = b$ ,

where  $A = I - \tau \tilde{A}$ ,  $b = u^n(\tilde{x})$  and  $x = u^{n+1}(\tilde{x})$ . Because of the local discretization method and the knowledge of the solvers we use the Multi-grid-solvers to solve our equation. For this type of a parabolic equation, confer [18], we could use the standard results.

We will briefly introduce the methods for a intensive study we refer to the literature [28], [27].

We deal with the linear equation-system

$$Ax = b, \quad A \in \mathbb{R}^{I \times I}, \quad b \in \mathbb{R}^I, \quad (45)$$

whereby  $A$  is regular,  $x$  is the unknown and  $b$  is the right hand side.

The iteration-method is given as :

$$x^{m+1} = Mx^m + Nb, \quad m \in \mathbb{N}, \quad (46)$$

whereby  $b$  is the right-hand side. and we get an consistent iteration-method for

$$M = \mathbb{1} - NA. \quad (47)$$

whereby  $\mathbb{1}$  is the identity matrix. The matrix  $M$  is denoted as iteration-matrix.

We could modify the equation (46) for the second normal-form given as

$$x^{m+1} = x^m - N(Ax^m - b). \quad (48)$$

The iteration-method is applied for the multi-grid method [18].

We introduce the multi-grid methods

$$M_0^{MG} := 0, \quad (49)$$

$$M_1^{MG} := M_1^{ZG}, \quad (50)$$

$$M_l^{MG} := M_l^{ZG} + S_l^{\nu_2} p (M_{l-1}^{MG})^\gamma A_{l-1}^{-1} r A_l S_l^{\nu_1}, \quad (51)$$

where  $S_l$  is the smoother,  $p$  is the prolongation,  $r$  is the restriction,  $\nu_1$  are the pre-smoothing steps and  $\nu_2$  the post-smoothing-steps. The coarse-grid correction  $M_l^{MGG}$  is defined as

$$M_l^{MGG} := \mathbb{1} - p (I - (M_{l-1}^{MG})^\gamma) A_{l-1}^{-1} r A_l. \quad (52)$$

We use these iteration-methods to solve our equations on a grid-hierarchy, confer [14].

In the next section we introduce our used software-tools.

## 7 Software-tools

The methods introduced in the last sections are programmed in our software-tool  $R^3T$ . The software package  $R^3T$  is developed for solving transport-reaction-equations for many species in flowing groundwater in a porous media. We forced the solution of convection-dominant equations and improved the discretizations to use coarser grids and larger time-steps. The package include the error-estimators, solvers and discretization methods. For the parameter of the equation and the velocity-field we use input-files to set the different values. These dates are read in run-time and for a new run we could change the values for a new configuration. The solutions of the equations are written in output-files and could be used for different post-processors, e.g. visualization-programs, confer Grape [17]. So for these assumption we could test different waste-case scenarios for different initial conditions, see section 8.

The tool  $R3T$  is based on the software-tool  $ug$ , confer [2], which is based on unstructured grid. The methods for these unstructured grids are programmed in different libraries. Based on the grid-hierarchy the solvers, e.g. multi-grid solvers, discretization-methods with respect of adaptive methods are programmed. The idea behind is a flexible tool with common libraries of solvers, discretization-methods, error-estimators and a flexible application-level for applications in physical- and chemical-models.

The application is presented in the next section with benchmark and waste-case scenarios.

## 8 Numerical experiments

The introduced methods in the last sections are verified in the first part. We compared the numerical results with analytical solutions.

In the next part we apply the improved modified methods to complex waste-case scenarios. An introduction to the test-cases in 2d and 3d are given and the results and computation time are discussed.

### 8.1 Benchmark-Problems

We compare the results of the standard method with the modified method.

The standard-method is based on the operator-splitting method with the convection- and reaction-equation. This method has a splitting error in time of  $O(\tau^n)$ .

The modified method is based on the discretization method with embedded analytical solutions for the convection-reaction equation. With this method we skip the splitting error in time.

We start with the one-dimensional problem and compare the results with the analytical solution.

**Transported triangle** For the first experiment we use a one-dimensional benchmark problem with delta initial conditions. The analytical solution is given by the equation (34) and (35) and compare the analytical solution with the numerical solutions.

We calculate the solutions on a 2 dimensional domain, for which the velocity field is constant in the x-direction with the constant value of  $\mathbf{v} = (1.0, 0.0)^T$ . We use only the convection-reaction equation with 4 components, given in the form

$$R_i \partial_t c_i + \mathbf{v} \cdot \nabla c_i = -R_i \lambda_i c_i + R_{i-1} \lambda_{i-1} c_{i-1}, \quad (53)$$

$$\text{with } i = 1, \dots, 4. \quad (54)$$

whereby the inflow/outflow boundary condition is given by  $\mathbf{n} \cdot \mathbf{v} c_i = 0.0$ , with no inflow and outflow. The initial condition is given as

$$c_1(x, 0) = \begin{cases} -x + 1, & 0 \leq x \leq 1 \\ 0, & \text{otherwise,} \end{cases} \quad (55)$$

$$c_i(x, 0) = 0.0, \quad i = 2, \dots, 4. \quad (56)$$

For the one-dimensional problem we could compare the numerical solutions with the analytical solutions derived in the previous sections. We use the  $L_1$ -norm to compare the solutions, which is given by

$$E_{L_1}^l := \sum_{i=1, \dots, m} V_i |c_i^n(x_j, y_j, t^n) - C_i(x_i, y_i, t^n)|, \quad \text{with } l = 1, \dots, 4, \quad (57)$$

where  $c_i^n(x_i, y_i, t^n)$  is the numerical solution while  $C_i(x_i, y_i, t^n)$  is the analytical solution, given in equation (34) and (35). The  $L_1$ -norm as an error-norm presents the errors of the convection-reaction equation in a good manner.

The model domain is given with an rectangle of  $8 \times 1$  units. The initial coarse grid is given with 8 quadratic unit elements, the uniform refinements are till the level 7 (131072 Elements).

We choose the parameters to get results at the end of the same maximum value, so that we would not see the influence of numerical effects with different scalars.

For the first test we use the following parameters:

We use the decay-rates of  $\lambda_1 = 0.4$ ,  $\lambda_2 = 0.3$ ,  $\lambda_3 = 0.2$ ,  $\lambda_4 = 0$  and the retardation factors  $R_1 = 1$ ,  $R_2 = 2$ ,  $R_3 = 4$ ,  $R_4 = 8$ .

The model time is done from  $t = 0, \dots, 6$ . We compared the results at the end-time  $t = 6$ . To do this we compared the  $L_1$ -norm and the numerical convergence-rate given by

$$\rho = (\log(E_{L_1}^l) - \log(E_{L_1}^{l-1})) / \log(0.5) \quad (58)$$

for the computed levels  $l = 4, \dots, 7$ .

The first results are presented with the standard method and the  $L_1$ -errors are given in the next Table 1.

The values for the numerical convergence-orders are denoted in the next Table 2.

| $l$ | $E_{L_1}^1$           | $E_{L_1}^2$           | $E_{L_1}^3$           | $E_{L_1}^4$           |
|-----|-----------------------|-----------------------|-----------------------|-----------------------|
| 4   | $2.666 \cdot 10^{-3}$ | $9.853 \cdot 10^{-4}$ | $9.77 \cdot 10^{-4}$  | $4.132 \cdot 10^{-4}$ |
| 5   | $1.297 \cdot 10^{-3}$ | $4.740 \cdot 10^{-4}$ | $4.805 \cdot 10^{-4}$ | $2.013 \cdot 10^{-4}$ |
| 6   | $6.148 \cdot 10^{-4}$ | $2.328 \cdot 10^{-4}$ | $2.377 \cdot 10^{-4}$ | $9.925 \cdot 10^{-5}$ |
| 7   | $2.969 \cdot 10^{-4}$ | $1.154 \cdot 10^{-4}$ | $1.181 \cdot 10^{-4}$ | $4.925 \cdot 10^{-5}$ |

**Table 1.** The  $L_1$ -errors computed with the standard method.

| $l$ | $\rho_{L_1}^1$ | $\rho_{L_1}^2$ | $\rho_{L_1}^3$ | $\rho_{L_1}^4$ |
|-----|----------------|----------------|----------------|----------------|
| 4   |                |                |                |                |
| 5   | 1.0394         | 1.0556         | 1.023          | 1.0374         |
| 6   | 1.077          | 1.0257         | 1.015          | 1.0202         |
| 7   | 1.0501         | 1.0124         | 1.009          | 1.0109         |

**Table 2.** The convergence-orders for the  $L_1$ -errors with the standard-method.

The results of the calculations are of the first order for all components. This consider the assumption of the splitting-error for the standard-method.

The next results are done with the modified method. We run the application with the same parameters as for the standard method. The  $L_1$ -errors for the modified method for the different time- and grid-widths are presented in the Table 3.

| $l$ | $E_{L_1}^1$           | $E_{L_1}^2$           | $E_{L_1}^3$           | $E_{L_1}^4$           |
|-----|-----------------------|-----------------------|-----------------------|-----------------------|
| 4   | $2.666 \cdot 10^{-3}$ | $3.451 \cdot 10^{-4}$ | $6.719 \cdot 10^{-5}$ | $2.376 \cdot 10^{-5}$ |
| 5   | $1.297 \cdot 10^{-3}$ | $1.072 \cdot 10^{-4}$ | $1.669 \cdot 10^{-5}$ | $5.573 \cdot 10^{-6}$ |
| 6   | $6.148 \cdot 10^{-4}$ | $3.374 \cdot 10^{-5}$ | $4.251 \cdot 10^{-6}$ | $1.374 \cdot 10^{-6}$ |
| 7   | $2.969 \cdot 10^{-4}$ | $1.117 \cdot 10^{-5}$ | $1.091 \cdot 10^{-6}$ | $3.442 \cdot 10^{-7}$ |

**Table 3.** The  $L_1$ -errors computed with the modified method.

The numerical convergence-orders for the modified method are calculated and presented in the Table 4.

For the first component we get the first order because of the space-discretization for the discontinuous impulse which is of first order. The results of the next components are of higher order. The error for the time-discretization is zero and for the space discretization we get a higher order because of the continuous impulses.

The results of the computations are presented in the end-time  $t = 6$  in figure 1. The first component is less retarded and is flown till the end of the interval. The next components are decreased stronger retarded and are therefore spreaded out. Because of the coupling with the previous component the next components

| $l$ | $\rho_{L_1}^1$ | $\rho_{L_1}^2$ | $\rho_{L_1}^3$ | $\rho_{L_1}^4$ |
|-----|----------------|----------------|----------------|----------------|
| 4   |                |                |                |                |
| 5   | 1.0394         | 1.686          | 2.009          | 2.092          |
| 6   | 1.077          | 1.667          | 1.973          | 2.0201         |
| 7   | 1.0501         | 1.594          | 1.962          | 1.997          |

**Table 4.** The convergence-orders for the  $L_1$ -errors with the modified-method.

are flown till the end of the first component. The last component is spreaded out from the first part of the interval till the end of the interval.

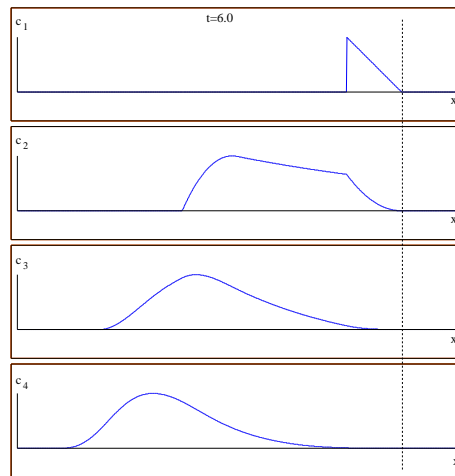


**Fig. 1.** Concentration for the 4 components with ascending retardation factors at time  $t = 6$ .

In the next section we will present a benchmark-problem for a 2 dimensional problem. We also derive the analytical solution.

**Rotating pyramid** This benchmark-problem is introduced in the literature as rotating Gaussian-impulse, confer [10]. To apply this problem also for system of convection-reaction-equations, we modify the problem for our derived analytical one-dimensional solutions. The modification is in the projection of the Cartesian-coordinates to the polar-coordinates. We could skip therefore one dimension and apply our one-dimensional solution. To be one-dimensional we project the initial conditions, which are triangles to the polar-coordinates. We get on each circle the same velocity and for the solution we could re-transform it to a one-dimensional problem.

The basic reconstruction is done in [14], we will present the ideas.

The transformation from the Cartesian to the polar-coordinates are given as

$$r = \sqrt{x^2 + y^2}, \alpha = \arctan\left(\frac{y}{x}\right), \epsilon(r) = r \alpha_0, \quad (59)$$

the  $(x, y) \in \mathbb{R} \times \mathbb{R}$  is the Cartesian coordinate, and  $r$  is the radius,  $\alpha$  is the angle for the origin point.  $\alpha_0$  is the initial-angle and  $\epsilon(r)$  is the length of the circular arc with radius  $r$ .

First we transform the triangular-impulse on the cylinder surface and get a continuous impulse.

Second we transfer the continuity in the  $r$ -direction with the dependency of the initial concentration  $c_0(r)$ . The transformation is given by

$$r_{med} = \frac{r_a + r_b}{2}, \quad (60)$$

$$c_0(r) = c_{init} \begin{cases} \frac{2}{r_b - r_a}(r - r_a) & r_a \leq r \leq r_{med} \\ \frac{2}{r_b - r_a}(r - r_b) & r_{med} \leq r \leq r_b \\ 0.0 & otherwise \end{cases}, \quad (61)$$

$$c_{init} \in \mathbb{R}^+, \text{ (initial-concentration).}$$

This initial impulse is then rotating with the angle  $\alpha$  in the domain. We calculate the length of the arc:

$$x_{arc}(r, \alpha) = r \alpha, \quad (62)$$

whereby  $r$  is the radius to the point  $(x, y)$  and  $\alpha$  the angle.

The velocity is given in the divergence-free form

$$\mathbf{v} = \begin{pmatrix} -4.0 y \\ 4.0 x \end{pmatrix}. \quad (63)$$

and it is given in the constant form in the polar-coordinates

$$v = 4.0 r, \quad (64)$$

The initialization for the rotating pyramid is given by

$$u_{1,init} = u_{1,Tri}(x_{arc}(r, \alpha_0), t_0, \epsilon(r), c_0(r), v_1, \lambda_1), \quad (65)$$

$$u_{i,init} = 0.0 \quad \text{with } i = 2, \dots, m, \quad (66)$$

whereby  $t_0 = 0.0$  and  $v_1 = \frac{v}{R_1}$  is denoted.  $m$  is the number of components and  $u_{1,Tri}$  is the analytical solution of a convection-reaction equation with a triangle-impulse.

The analytical solution for an arbitrary time is given as :

$$u_{i,Tri} = u_{i,Tri}(x_{arc}(r, \alpha), t, \epsilon(r), c_0(r), v_1, \dots, v_i, \lambda_1, \dots, \lambda_i), \quad (67)$$

whereby  $i = 1, \dots, m$  and  $v_i = \frac{v}{R_i}$ .

We compute the example for 4 components. The retardation-factor are  $R_1 = 1.0$ ,  $R_2 = 2.0$ ,  $R_3 = 4.0$ ,  $R_4 = 8.0$  and the reaction-factors are  $\lambda_1 = 1.5$ ,  $\lambda_2 = 1.4$ ,  $\lambda_3 = 1.3$ ,  $\lambda_4 = 0.0$ . The height of the pyramid is  $c_{init} = 1$ , the base area of the pyramid is the radius  $0.125 \leq r \leq 0.375$  and the initial-angle  $\alpha_0 = 0.22$ . The next components are initialized with 0.0. The boundary conditions are trivial inflow- and outflow-conditions. We have a domain with  $[-0.5, 0.5] \times [-0.5, 0.5]$  and the coarse grid consists of one element. We maximal refine till grid-level 7. The time-steps are fixed for level and fulfill the Courant-number 0.5. We calculate till the end-point  $t = \pi/4$ .

For the modified method we get the results in Table 5 for the  $L_1$ -error and the convergence-rates.

| $l$ | $E_{L_1}^1$          | $\rho_{L_1}^1$ | $E_{L_1}^2$          | $\rho_{L_1}^2$ | $E_{L_1}^3$          | $\rho_{L_1}^3$ | $E_{L_1}^4$          | $\rho_{L_1}^4$ |
|-----|----------------------|----------------|----------------------|----------------|----------------------|----------------|----------------------|----------------|
| 4   | $7.12 \cdot 10^{-3}$ |                | $5.80 \cdot 10^{-4}$ |                | $3.09 \cdot 10^{-5}$ |                | $8.28 \cdot 10^{-7}$ |                |
| 5   | $2.74 \cdot 10^{-3}$ | 1.377          | $2.14 \cdot 10^{-4}$ | 1.44           | $1.12 \cdot 10^{-5}$ | 1.46           | $2.86 \cdot 10^{-7}$ | 1.53           |
| 6   | $1.10 \cdot 10^{-3}$ | 1.32           | $8.82 \cdot 10^{-5}$ | 1.27           | $4.90 \cdot 10^{-6}$ | 1.19           | $1.20 \cdot 10^{-7}$ | 1.25           |
| 7   | $4.40 \cdot 10^{-4}$ | 1.322          | $3.50 \cdot 10^{-5}$ | 1.33           | $1.90 \cdot 10^{-6}$ | 1.37           | $4.80 \cdot 10^{-8}$ | 1.32           |

**Table 5.** The  $L_1$ -error and the convergence-rate for modified method with embedded analytical solution

For all components we reach the higher order results because of the modified method.

The results are presented in the figure 2. In the first figure we present the initialization in the next figure we present the end-result.

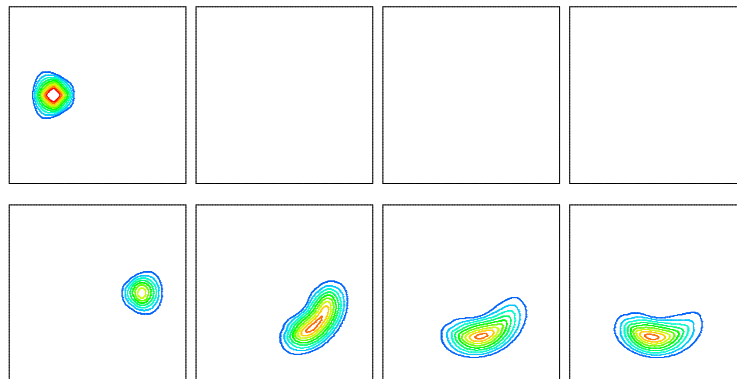


**Fig. 2.** The concentrations of the 4 components at the time-point  $t = \frac{\pi}{4}$ .

The concentrations of the higher components are stronger retarded. The first component is furthest transported and rotated till the half of the circle. The previous components are spread out till the following components. The two dimensional solutions also fulfill our theoretical results.

In the next section we present the complex waste case scenarios of a waste-disposal done in a salt-dome.

## 8.2 Waste-Case Scenarios

We calculate scenarios of waste-cases which help to get new conclusions about the waste-disposals in salt-domes.

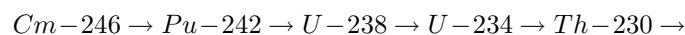
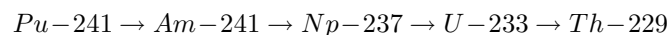
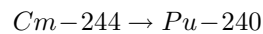
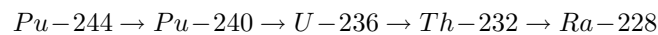
We have a model based on an overlying-rock over a salt-dome. We suppose an waste-case, so that a permanent source of radioactive contaminant groundwater flow from the bottom of the overlying rock, where the waste-disposal is suited. We suppose that the contaminants are flown with the groundwater, which is flown through the overlying rock. Based on our model we should calculate the transport and the reaction of this contaminants coupled with decay-chains. The simulation time should be  $10000[a]$  and we should calculate the concentration that is flown till the top of the overlying rock. With this dates one could conclude if the waste-disposal is save enough.

Two cases are next presented with the dates of our project-partner GRS in Braunschweig (Germany), confer [7] and [8].

## 8.3 First waste-case : Two Dimensional Model

We have a model-domain in the size of  $6000[m] \times 150[m]$  with 4 different layers with different permeabilities, [7]. The domain is spooled with groundwater from the right boundary to the left boundary. The groundwater is flowing faster through the permeable layer as through the impermeable layers. Therefore the groundwater flows from the right boundary to the half middle of the domain. Flowing through the permeable layer down to the bottom of the domain and spooled up in the left domain to the top. The groundwater flows in the left top part to the outflow at the left boundary. The flow-field with the velocity is calculated with the program-package **d<sup>3</sup>f** and presented in figure 3.

In the middle-bottom of the domain the contaminants are flown in as a permanent source. With the stationary velocity-field the contaminants are computed with the software-package  $R^3T$ . The flow-field transport the radioactive contaminants till the top of the domain. The decay-chain is presented with 26 components as follows



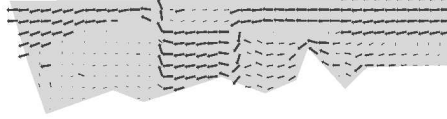
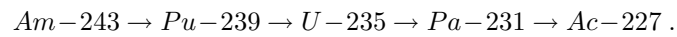
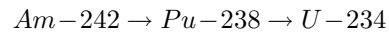
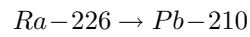


**Fig. 3.** Flow-field for a two-dimensional calculation.



We present the important concentration in this decay-chain. In the top figure 4 the contaminant Uran-isotope U-236 after 100[a] is presented. This isotope is less retarded and has a very long half-life period. Therefore the contaminant is flown as furthest and decay less. This effect is presented in bottom figure 4. The diffusion-process has spread out the contaminant in the whole left part of the domain. Also the impermeable layer is contaminated. After the time-period of 10000[a] the contaminant is flown till the top of the domain.

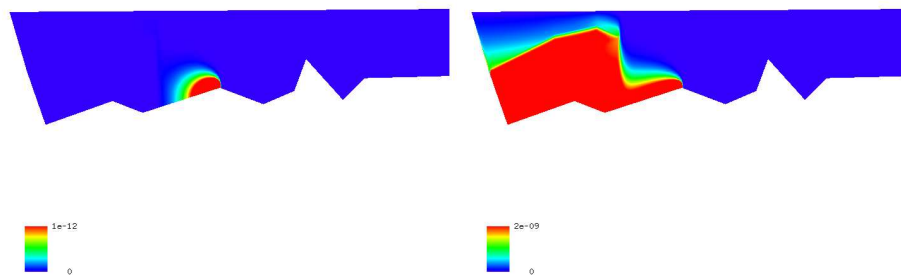


**Fig. 4.** Concentration of U-236 at the time-point  $t = 100[a]$  and  $t = 10000[a]$ .

The calculations are done on uniform grids. The convergence of this grids are confirmed with adaptive grid-calculations. The calculation confirmed the results of finer and smaller time-steps, confer Table 6. The beginning of the calculations are done with explicit methods till the character of the equation is more diffusive. Then we change to the implicit methods and could use larger time-steps. With this procedure we could fulfill the forced calculation time of maximal one day.

| Processors | Refinement | Number of Elements | Number of Time-steps | Time for one time-step | Total Time |
|------------|------------|--------------------|----------------------|------------------------|------------|
| 30         | uniform    | 75000              | 3800                 | 5 sec.                 | 5.5 h.     |
| 64         | adaptive   | 350000             | 3800                 | 14 sec.                | 14.5 h.    |

**Table 6.** Computing of the two-dimensional case.

In the next section we describe our three dimensional test-case.

#### 8.4 Second waste-case : Three Dimensional Model

In this model we calculate a three dimensional model, because of the interest for the three dimensional effects in the flowing groundwater. We simulate about 10000[a] and concentrate us to important contaminants flown furthest with a high rate of concentration. We underly an anisotropy domain of  $6000[m] \times 2000[m] \times 1500[m]$  with different permeable layers. We have calculated 26 components as presented in the two dimensional case. The parameters for the diffusion and dispersion-tensor are given as:

$$D = 1 \cdot 10^{-9} [m^2/s] , \alpha_L = 4.0 [m] , \alpha_T = 0.4 [m], |v|_{max} = 6 \cdot 10^{-6} [m/s], \rho = 2 \cdot 10^3 .$$

$$D_L = \alpha_L |v| \text{ and } D_T = \alpha_T |v| ,$$

whereby the longitudinal dispersion length is 10 times bigger than the transversal dispersion. The source are suited at the point (4250.0, 2000.0, 1040.0) and is flown in with a constant rate. The underlying velocity-fields is calculated with  $d^3 f$  and we added to sinks at the surface with the coordinates (2000, 2100, 2073) and (2500, 2000, 2073).

We simulate the transport and the reaction of the contaminants with our software-package  $R^3T$ . Therefore we could test how strong should be the sinks at the top of the domain to bring out the contaminant groundwater. We present the velocity-field in figure 5. The groundwater is flown form the right boundary to the middle of the domain. Due to the impermeable layers the groundwater is flown down and spooled up in the middle part of the domain. The groundwater is flown up to the sinks in the left part at the top of the domain. Because of the influence of the salt-dome the salt is spooled up with the groundwater and we get in the lower middle part of the domain curls. This parts are interested for 3d calculations and due to this curls the groundwater is spooled up. We concentrate

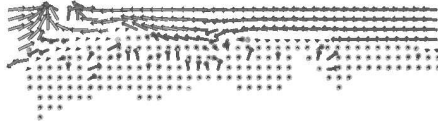


**Fig. 5.** Flow-field for a three-dimensional calculation.

us to the important component  $U - 236$ . This component is less retarded and is flowing up to the earth-surface into the sinks. In the top figures 6 we present the concentration in the initial-concentration at time point  $t = 100 [a]$ . We have present cut-planes vertical and in the next picture a cut-plane through the source term. In the bottom figure 6 the concentration is presented at the end-time point  $t = 10000 [a]$ . The concentration is flown from the bottom up over the impermeable layer into the sinks at the top of the domain.

At the beginning of the calculation we use explicit discretization methods with respect of the convection-dominant case. After the initializing process the contaminants are spreaded out with the diffusion-process. We use the implicit methods with larger time-steps and could calculate the forced time-period also in a higher order discretization.

In the Table 7 we denote the computations. We begin with convergence results on uniform refined meshes. We confirm this results with adaptive refined meshes and get the same results with smaller time-steps. The forced calculation-time of one day is fulfilled.

| Processors | Refinement | Number of elements | Number of time-steps | time for one time step | total time |
|------------|------------|--------------------|----------------------|------------------------|------------|
| 16         | uniform    | 531264             | 3600                 | 13.0 sec.              | 13.0 h     |
| 72         | adaptive   | 580000             | 3600                 | 18.5 sec.              | 18.5 h     |

**Table 7.** Three dimensional calculations of a realistic potential damage event.

Finally we conclude in our paper with the next section.

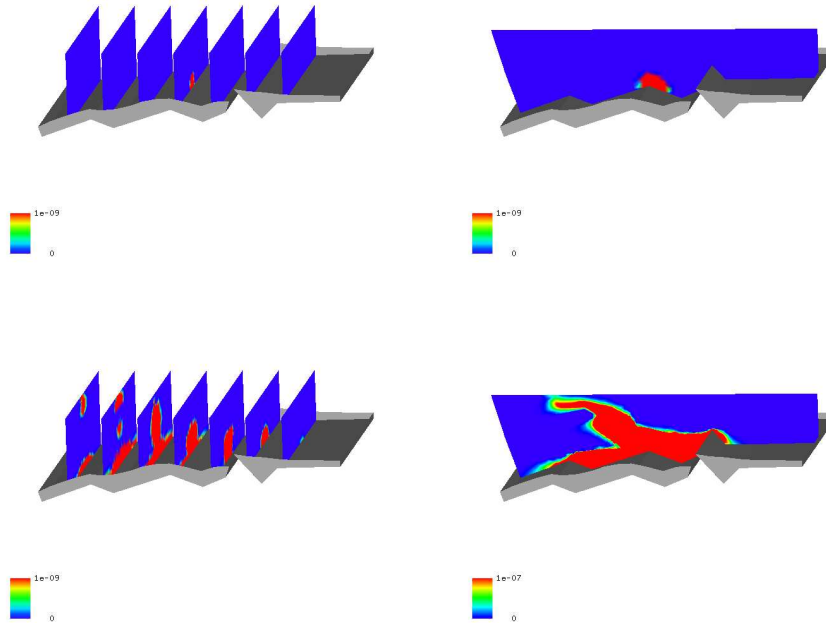


**Fig. 6.** Concentration of U-236 at the time-point  $t = 100[a]$  and  $t = 10000[a]$ .

## 9 Conclusions and Discussions

We present a discretization methods to solve a complex system of convection-diffusion-dispersion-reaction equation. Based on a new technic of embed analytical solution we improve the standard discretization methods. The splitting methods are described and the applications of our methods are presented. We could explain our solvers and the based program-tool. The test-examples and the complex waste-scenarios are presented.

We could confirm that a complex model could be simulated with the help of different splitting and discretization methods.

In the future we focus us on the development of improved discretization methods and the idea of decoupling in simpler equations with respect to nonlinear convection-diffusion-reaction-equations.

## References

1. M. Abramowitz, I.A. Stegun. *Handbook of Mathematical Functions*, Dover Publication New York, 1970;

2. P. Bastian, K. Birken, K. Eckstein, K. Johannsen, S. Lang, N. Neuss, and H. Rentz-Reichert. *UG - a flexible software toolbox for solving partial differential equations*. Computing and Visualization in Science, 1(1):27–40, 1997.
3. H. Bateman. *The solution of a system of differential equations occurring in the theory of radioactive transformations*. Proc. Cambridge Philos. Soc., v. 15, pt V:423–427, 1910.
4. B. Davis. *Integral Transform and Their Applications*. Applied Mathematical Sciences, 25, Springer Verlag, New York, Heidelberg, Berlin, 1978 .
5. G.R.. Eykolt. *Analytical solution for networks of irreversible first-order reactions*. Wat.Res., 33(3):814–826, 1999.
6. E. Fein, T. Kühle, and U. Noseck. Entwicklung eines Programms zur dreidimensionalen Modellierung des Schadstofftransportes. *Fachliches Feinkonzept* , Braunschweig, 2001.
7. E. Fein. *Test-example for a waste-disposal and parameters for a decay-chain*. Private communications, Braunschweig, 2000.
8. E. Fein. *Physical Model and Mathematical Description*. Private communications, Braunschweig, 2001.
9. P. Frolkovič and J. Geiser. *Numerical Simulation of Radionuclides Transport in Double Porosity Media with Sorption*. Proceedings of Algorithmy 2000, Conference of Scientific Computing, 28-36, 2000.
10. P. Frolkovič. *Flux-based method of characteristics for contaminant transport in flowing groundwater*. Computing and Visualization in Science, 5(2):73–83, 2002.
11. P. Frolkovič and J. Geiser. *Discretization methods with discrete minimum and maximum property for convection dominated transport in porous media*. Proceeding of NMA 2002, Bulgaria, 2002.
12. P. Frolkovič and H. De Schepper. *Numerical modelling of convection dominated transport coupled with density driven flow in porous media*. Advances in Water Resources, 24:63–72, 2001.
13. J. Geiser. *Numerical Simulation of a Model for Transport and Reaction of Radionuclides*. Proceedings of the Large Scale Scientific Computations of Engineering and Environmental Problems, Sozopol, Bulgaria, 2001.
14. J. Geiser. *Discretisation methods for systems of convective-diffusive-dispersive-reactive equations and applications*. Doctor Thesis, University of Heidelberg, Germany, 2004.
15. J. Geiser. *R<sup>3</sup>T : Radioactive-Retardation-Reaction-Transport-Program for the Simulation of radioactive waste disposals*. Proceedings: Computing, Communications and Control Technologies: CCCT 2004, The University of Texas at Austin and The International Institute of Informatics and Systemics (IIIS), to appear, 2004.
16. M.Th. Genuchten. *Convective-Dispersive Transport of Solutes involved in sequential first-order decay reactions*. Computer and Geosciences, 11(2):129–147, 1985.
17. GRAPE. *GRAphics Programming Environment for mathematical problems, Version 5.4*. Institut für Angewandte Mathematik, Universität Bonn und Institut für Angewandte Mathematik, Universität Freiburg, 2001.
18. W.Hackbusch. *Multi-Grid Methods and Applications*. Springer-Verlag, Berlin, Heidelberg, 1985.
19. K. Higashi und Th. H. Pigford. *Analytical models for migration of radionuclides in geologic sorbing media*. Journal of Nuclear Science and Technology, 17(9):700–709, 1980.
20. W.H. Hundsdorfer. *Numerical Solution od Advection-Diffusion-Reaction Equations*. Technical Report NM-N9603, CWI, 1996.

21. W.A. Jury, K. Roth. *Transfer Funktionen and Solute Movement through Soil*. Birkhäuser Verlag Basel, Boston, Berlin, 1990 .
22. R.J. LeVeque. *Finite Volume Methods for Hyperbolic Problems*. Cambridge Texts in Applied Mathematics ,
23. A.E. Scheidegger. *General theory of dispersion in porous media*. Journal of Geophysical Research, 66:32–73, 1961.
24. G. Strang. *On the construction and comparison of difference schemes*. SIAM J. Numer. Anal., 5:506–517, 1968.
25. Y. Sun, J.N. Petersen and T. P. Clement. *Analytical solutions for multiple species reactive transport in multiple dimensions*. Journal of Contaminant Hydrology, 35:429–440, 1999.
26. J.,G. Verwer and B. Sportisse. *A note on operator splitting in a stiff linear case*. MAS-R9830, ISSN 1386-3703, 1998.
27. G. Wittum. *Multi-grid Methods : A introduction*. Bericht 1995-5, Institut für Computeranwendungen der Universität Stuttgart, Juni 1995.
28. H. Yserentant. *Old and New Convergence Proofs for Multigrid Methods*. Acta Numerica, 285–326, 1993.
29. Z. Zlatev. *Computer Treatment of Large Air Pollution Models*. Kluwer Academic Publishers, 1995.